LANGMUIR-BLODGETT ASSEMBLY OF YEAST CELLS AND COLLOIDAL PARTICLES

By

HEMALATHA VELAVAN

A THESIS PRESENTED TO THE GRADUATE SCHOOL
OF THE UNIVERSITY OF FLORIDA IN PARTIAL FULFILLMENT
OF THE REQUIREMENTS FOR THE DEGREE OF
MASTER OF SCIENCE

UNIVERSITY OF FLORIDA

2013

To amma and appa

ACKNOWLEDGMENTS

First and foremost I would like to thank my advisor Dr.Peng Jiang for his patience and advice. I would like to thank my committee members Dr.Kirk Zeigler and Dr.Yiider Tseng for their suggestions and inputs. I also thank Shan, Blayne, Khalid, Baeck and Numan for their help with different issues. I would also like to thank my friends and roommates for standing by me during testing times.

TABLE OF CONTENTS

page

LIST OF TABLES

LIST OF FIGURES

LIST OF ABBREVIATIONS

ETPTA	Ethoxylated trimethylolpropane triacrylate
NaOH	Sodium hydroxide
Nm	nanometers
PANI	Polyaniline
PDMS	Polydimethylsiloxane
PEGDA	Polyethylene glycol diacrylate
SEM	Scanning Electron Microscope
UV	Ultraviolet
wt	weight

Abstract of Thesis Presented to the Graduate School
of the University of Florida in Partial Fulfillment of the
Requirements for the Degree of Master of Science

LANGMUIR-BLODGETT ASSEMBLY OF YEAST CELLS AND COLLOIDAL PARTICLES

By

Hemalatha Velavan

May 2013

Chair: Peng Jiang
Major: Chemical Engineering

The research objective of the project has two parts and both are related to fabrication using floating assembly. The first part describes a simple and efficient method of coating of live cells. Live cell colloidal coatings have numerous applications in research labs as well as diagnostic labs. A simple and inexpensive coating of cells can be prepared by manipulating a floating assembly of cells at air/water interface. The coatings formed are analyzed to optimize the number of coatings, operating conditions and also the concentration of the colloidal solution used to form the floating cell assembly. The coating methodology is demonstrated using yeast but it can be said that the same procedure can be applied to various other cells and other biological macromolecules as required by the application.

The second part describes a simple and inexpensive method for fabrication of antireflection coating also using floating assembly. Various lithography techniques used in creating 200nm features for moth eye structure fabrication suffer from various limitations including high cost and low resolution. By using dip coating to fabricate the biomimetic coatings we decrease the cost and time of preparation. PDMS master templates are created using glass substrates dip coated silica nanoparticles. PDMS that

have the 200nm particles embedded on their surface are later manipulated in two different ways to fabricate dimple and nipple structures on ETPTA supported on glass substrate. The structures are fabricated on single side and both sides of the glass substrate and are examined for their optical properties.

CHAPTER 1
INTRODUCTION

Floating Assembly

Floating assembly has recently been exploited to fabricate desired materials ranging from free-floating particulate sheets (1) to Three-dimensional (3D) cell scaffolds (2). Nanoparticles have been shown to have the ability to self-assemble into well organized structures (3-5). Floating self assembly is a practical, fast and easy organization process for fabricating nanostructures. These floating assemblies have been used for depositing particles such as gold nanoparticles(6), zeolites(7) , biological polymers such as enzymes (8) and electrical conductors such as polyaniline (PANI)(9).Such depositions or coatings prepared by exploiting the floating assembly structure can be used to develop clean fuel from different energy and electron sources (10), self-cleaning or antifouling cell coatings (11), and industrial biocatalytic coating (12) etc.

Dip Coating

One of the easiest methods that utilize the free floating characteristic of small particles including microbes and nanoparticles is the dip coating methodology. Objects of any shape ranging from flat planes to complex cubes or sphere like structures can be coated with the desired particles under optimum conditions (13). The dip coating process is said to have five stages: immersion, start up, deposition, drainage and evaporation. A total of 6 forces account for the coating phenomenon and they act on various regions. Viscous drag force acts on the substrate, in this case the glass that is moving upward. Surface tension acts on the meniscus of the solvent. Gravity acts on all the components. Boundary layer inertial force can be seen on the area where the

particles are getting precipitated on the substrate. Surface tension gradient and pressure are significant on films of low thickness (14). The pressure is notable in the case of the 200nm particles but is not significant in the case of multilayer of yeast but may play a key role in monolayer depositions. The dip coating process has various advantages such as low cost, high adherence of particles, absence of seam lines on end product and ease of coating. The process is generally widely used in research and also in industries to deposit metals, minerals, plastisol, and epoxy on to tools, furniture and equipments made up of metals, glass and silica.

Spin Coating

A thin uniform film of polymer is generally coated using spin coating technique (15). The equipment commercially available for spin coating is called a spinner or a spin coater. The process involves spreading of fluid on substrate due to the centrifugal force applied by the spin coater. The polymer is poured on the substrate that is placed at the centre of the coater and allowed to spread across its surface. The polymer can be added in excess or in drops depending on the thickness required. The spinning is set at an optimum speed for a specific duration to get the desired thickness. After the process the polymer is either baked at high temperature or cured under UV light. Major advantages of spin coating include the short duration for fabrication, low cost and uniformity in the coat produced. Since there is a lid that protects the sample being processed from atmospheric disturbances the process conditions suffer very few variations. Compared to dip coating, spin coating is widely applied in industries especially for photolithography and microfabrication. Spin coating is generally used in the manufacturing of compact discs, television tubes, microcircuits and flat screen displays.

Biomimetic Antireflection Coating

Antireflection coatings (ARCs) are coating fabricated or coated over surface of materials to reduce their reflection. These materials are generally lenses or parts of optical systems or any system that requires light energy to function. The antireflection coatings help to increase the efficiency of the system by reducing the amount of light lost. Generally, antireflection coatings can be of two types: interference coating or textured coating. The nanofabricated coatings discussed here are textured coatings as they are characterized by nipples and dimples in nanometer scale. Many of textured antireflection coatings have been inspired by examples found in nature.

Micro and nanostructures have been an inspiration to mankind to fabricate different materials used for practical applications (16-19). '*Morpho*' butterflies have metallic blue or green shimmering on their wings which is due to iridescence due to the nanostructures generally referred to as microscopic scales. These structures are arranged such that they form tetrahedral layers that act like photonic crystals. These butterfly wings have become models for designing fabrics, sensors, paints etc. Insects like moths have nanostructures in their eyes that act as antireflection coatings (ARCs). These structures are nothing but sub 300nm nipples that reduce reflectivity to help them see during night time (20). Inspired by moth-eye ARCs many day to day gadgets have been fitted with artificially made ARCs ranging from solar cells to computer screens (21-24).

There are different types of anti reflection coatings such as polyelectrolyte coatings, nanoporous coating etc. But all these have several limitations in terms of scalability, cost and performance (25, 26). Techniques like photolithography, interference lithography and other top down microfabrication techniques have been

used for fabricating sub 300nm structures but they have also face major problems like high cost, low resolution, difficulty in scale up and small sample size (27). Thus, in this project we combine simple yet highly scalable dip coating technique in combination with spin coating bottom up self assembly techniques that utilize floating assembly to fabricate the 200nm features on to the polymer supported by glass slide. One of the important factors being able to use the PDMS mold as a master template to reproduce the 200nm features repeatedly.

CHAPTER 2
FLOATING ASSEMBLY OF YEAST CELLS

Experiment

Preparation of Yeast Cell Suspension

The schematic outline of the process is shown in Figure 2-1. The yeast cell suspension is prepared by dispersing 0.5g of Fleischmann's active dry yeast, *Saccharomyces cerevisiae* (ACH Food Companies, Memphis, TN) in 10ml of deionised water. The yeast cells are sprinkled over the water and left undisturbed in room temperature for about 5 min. The yeast cells are suspended well using a vortex mixer and the suspension is incubated at room temperature without any disturbances.

The pH of the suspension is measured using a pH test paper and is adjusted to 8.0 using cell culture tested 1.0 N NaOH (Sigma-Aldrich). The pH is consistently maintained at 8.0 as the yeast cells grow by adding small aliquots of 1N NaOH every 30 min. The yeast suspension is centrifuged at 3500 rpm for 5 min. The supernatant is discarded and ethylene glycol (ARCOS Organic) is added to prepare 20 wt %, 30 wt % and 40 wt % of suspension of yeast cells. The suspension is mixed well using a vortex mixer. Prior to setting up the floating assembly the cell suspension is sonicated for 15 – 20s to break up aggregates.

Set Up and Coating Fabrication

Glass microslides (Fisher) are cleaned and rinsed with milli-Q water (18.2 MΩ cm) and dried in a stream of air. A cleaned microslides is taped to the syringe pump on one end such that the other end is dipped into a beaker of deionized water. The set up is maintained in an air flow free place to prevent disturbances. The set up is left undisturbed for 10 min to minimize fluctuations on the water surface. A fiber optic light is

used to light the water-air interface. The suspension is gently added drop wise along the walls of the beaker to prevent surface fluctuations. After the water surface is completely covered with yeast cells the set up is left undisturbed for a 10 min. When the syringe pump is switched on the film won the water-air interface is transferred to glass as the glass slide is slowly pulled out of the beaker at a lifting speed of 50μm/min. The same steps are repeated twice and thrice for different suspension concentrations.

Image and Data Analysis

80 images were taken randomly from each sample using an optical microscope. A Java based image processing software named 'ImageJ' (Wayne Rasband, National Institute of Mental Health) is used to process the images to estimate area covered by yeast cells. In general, ImageJ calculates area and pixel value statistics of the desired domains in the images provided for processing. The images are manipulated using various tools to adjust issues like threshold, color and area of interest. Using the built-in function 'Analyze particles' the coverage percentage is estimated after processing the images to get the desired adjustments.

The percentage coverage obtained is analyzed with respect to the number of coatings and the concentration of the yeast suspension.

Results and Discussion

Image Analysis

As mentioned before eighty images were taken from each sample. Three images of each slide is shown in the following pages for simplicity and ease of comparison. But for the data analysis all the images that were taken are taken into account.

Figure 2-2 shows the images taken from glass slides coated with 20% suspension of yeast. Figure 2-2 A shows three images each of them depicting slides

subjected to dip coating once. Similarly Figure 2-2 B and Figure 2-2C show slides coated with 20% yeast suspension twice and thrice respectively. It is easily seen that the percentage coverage is low in the slides coated once. Moreover, the cells are not deposited uniformly but are seen to be deposited in specific areas. Figure 2-2 B shows better coverage but still cells are deposited in certain domains and large parts of the slides remain uncovered. Figure 2-2 C shows three slides having more than three-forth of its surface covered but still we are able to see small uncovered areas.

Figure 2-3 are images of yeast slides that were coated using 30% yeast suspension. As in the previous case, Figure 2-3 A, Figure 2-3 B, Figure 2-3 C are glass slides coated with yeast suspension once, twice and thrice respectively. Figure 2-3 A shows low coverage but the cells are spread out and almost evenly deposited in a monolayer all over the slide. When compared to Fig 2-2A it can be said that there are few large unoccupied domains. In case of Figure 2-3 B a better coverage is shown when compared to Figure 2-3 A. Moreover, when we compare with the twice coated 20% yeast suspension, slide depicted in Figure 2-2B, it can be seen that the unoccupied domains are still present but the empty domains are not only low in number but also smaller in size. Figure 2-3 C showing thrice coated slide have a relatively larger area of coverage and when compared with Figure 2-2C it can be seen the unoccupied domains are very small and also the area of coverage is better. There may be multiple layers in few areas.

The 40% yeast suspension coated slides are shown in Figure 2-4. Figure 2-4 A, showing slide dip coated once with 40% yeast suspension, is similar to Figure 2-3 A. Like the slides coated once with 30% yeast suspension, the cells are well dispersed and

there are very few large unoccupied domains. But it can also be noticed that in comparison there are relatively more empty domains than Figure 2-3 A. But in comparison to slides coated once with 20% yeast suspension the area covered is better. Figure 2-4 B shows very high area coverage when compared to Figure 2-2B as well as Figure 2-3 B. There are very few empty domains when compared to the slides coated by 20% and 30% yeast suspension. Relatively very less space is left unoccupied in Figure 2-4 C. It is also suspected that more multiple cell layers are present when compared to the 30% thrice coated slides.

Image Processing and Data Analysis

Images processed, using 'ImageJ' software, were used to analyze the percentage coverage of yeast cells. The images shown in Figure 2-5 are of 30% twice coated slides. These images are shown as samples to depict the processed and unprocessed images. All the images that were taken for the experiment were subjected to the same processing steps as the images depicted. Figure 2-5A is the raw image obtained from the optical microscope and Figure 2-5B depicts its processed image after its threshold and color being adjusted. Similarly, Figure 2-5C is a raw image and Figure 2-5D is its corresponding processed image. The processed images were then analyzed using the built-in 'Analyze particles' tool to get area covered in exact percentage.

The Table-2-1 shows the percentage area covered by yeast cells dip coated on to glass slides using 20%, 30% and 40% yeast cell suspension. It shows the data for one, two and three coatings. It is seen in the 20% data set that there is around 47% increase in percentage area from one coat to single coated. When coated thrice there is an increase an area covered from 54.21% to 68.50%. When 30% yeast cell suspension slides are considered, the percentage coverage between one coating and two coating

slides shows a significant increase. The 40% yeast suspension slides shows the most significant rise in percentage coverage between single and double coats. But there is a very less relative increase in percentage cell coverage from double coats (82.98%) to triple coats (86.85%). The data given in the table is plotted as a graph to show the percentage area coverage.

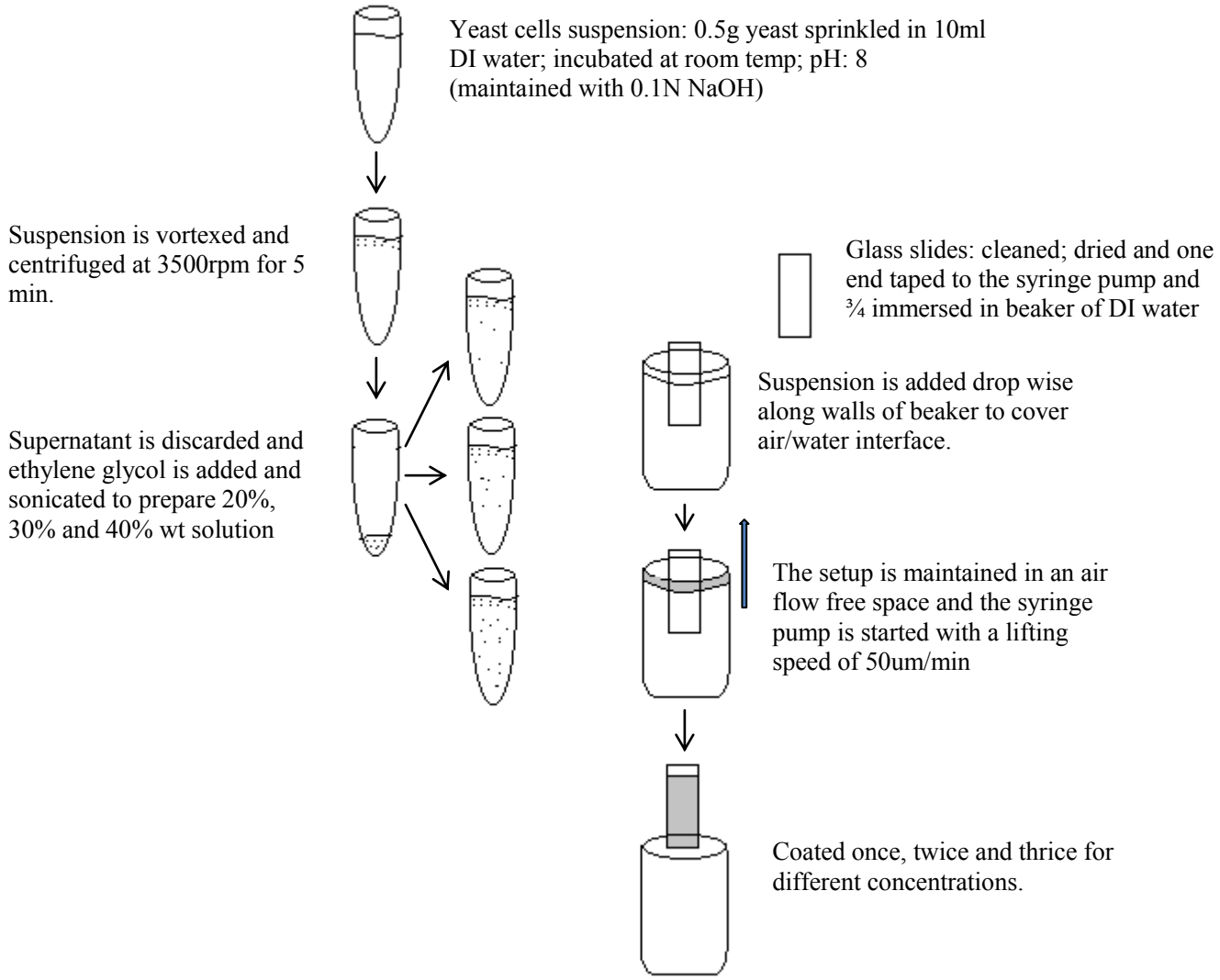

Figure 2-1. Fabrication of yeast cell coatings using floating cell assembly

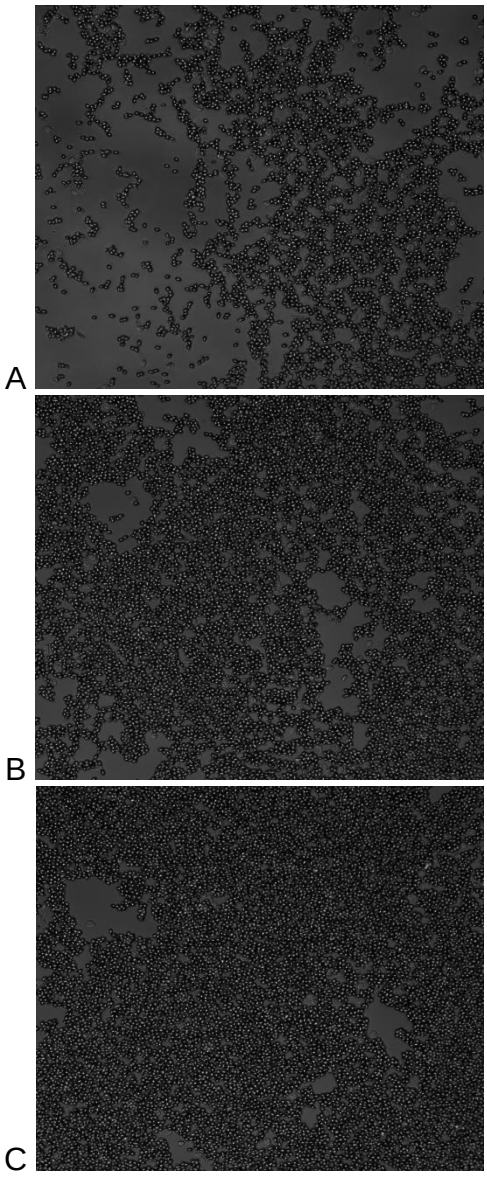

Figure 2-2. Glass dip coated with 20% yeast suspension. A) Slide coated once, B) Slide coated twice, C) Slide coated thrice.

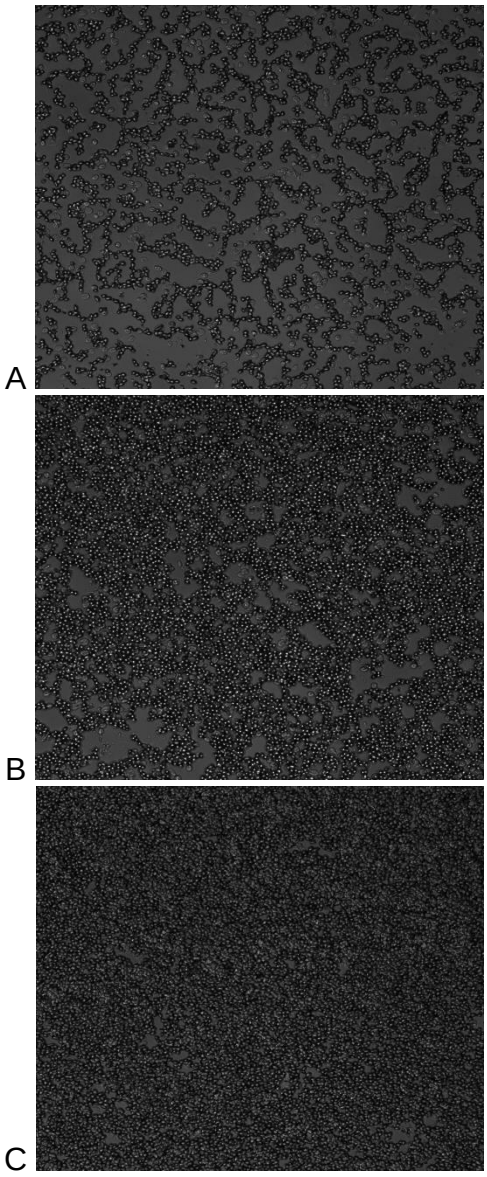

Figure 2-3. Glass dip coated with 30% yeast suspension. A) Slide coated once, B) Slide coated twice, C) Slide coated thrice.

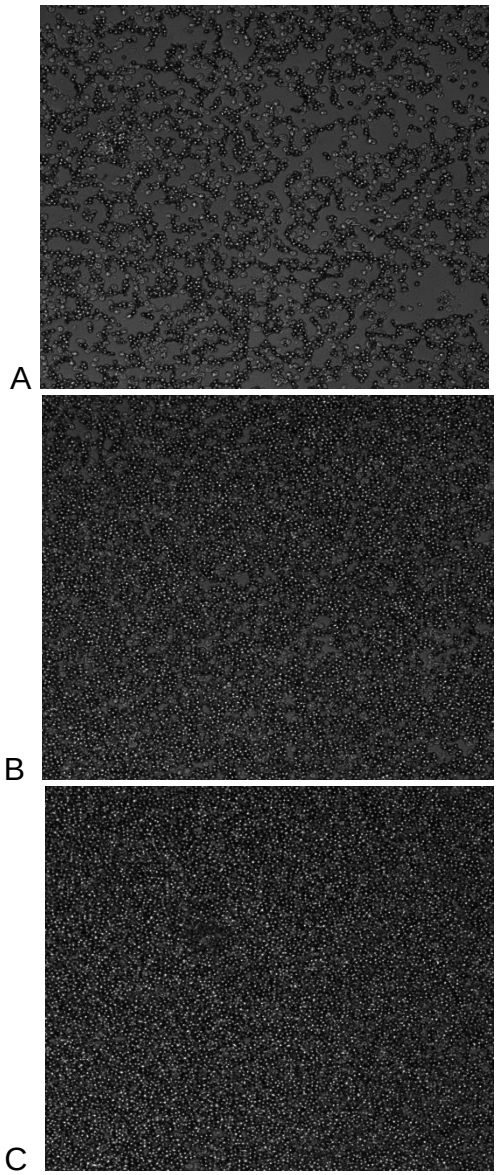

Figure 2-4. Glass dip coated with 40% yeast suspension. A) Slide coated once, B) Slide coated twice, C) Slide coated thrice.

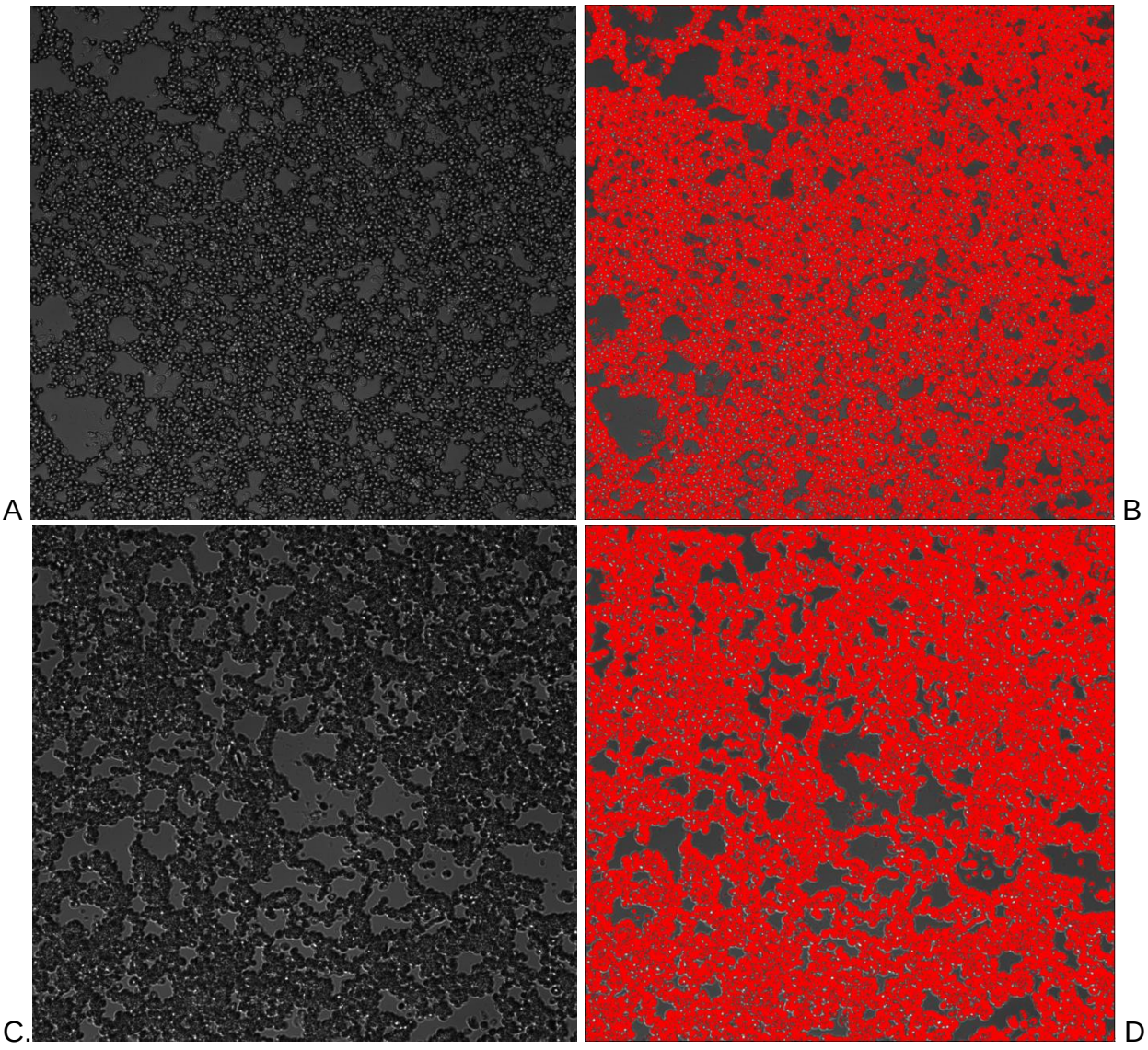

Figure 2-5. Images of twice coated with 30% yeast twice, processed using 'ImageJ' software. A) Unprocessed raw image, B) Corresponding processed image, C) Unprocessed raw image, D) Corresponding processed image.

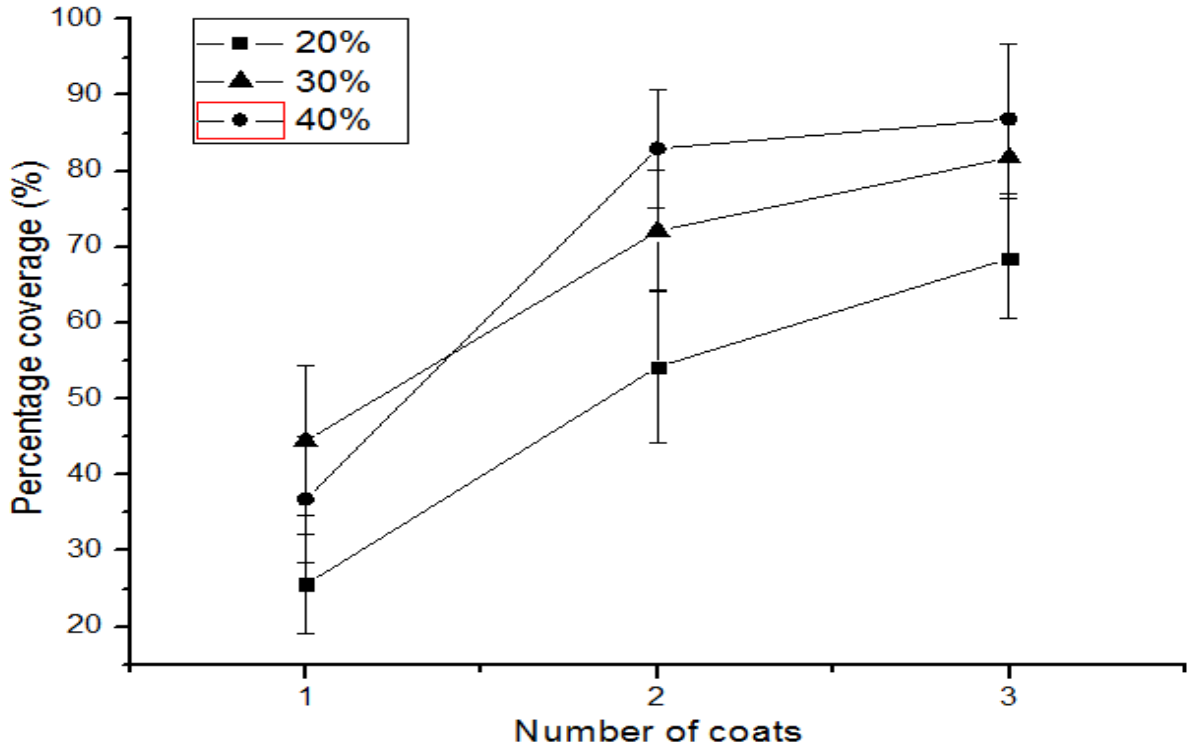

Figure 2-6. Graph showing percentage coverage vs. number of coats

Table 2-1. Percentage covered by yeast on slides

Number of coats	Percentage coverage					
	20%		30%		40%	
1	25.26	6.58	44.47	9.82	36.77	8.27
2	54.21	10.08	72.10	8.03	82.98	7.82
3	68.50	7.85	81.80	5.33	86.85	9.89

CHAPTER 3
BIOMIMETIC ANTIREFLECTION COATINGS

Experiment

Preparation of 200nm Particles

The fabrication of close-packed colloidal crystals is done on glass substrate using dip coating technology. The major advantage of this technique is that it is an easy and reproducible method to prepare samples in large scale in a short span of time.

200nm silica particles are purified with ethanol to remove the ammonium hydroxide that it is suspended in. The particles are then mixed with ethylene glycol and mixed well using a sonicator to suspend the particles uniformly. For every 1g of silica particles 10ml of ethylene glycol is added and mixed. The particles are covered in aluminum foil to prevent exposure to light.

Dip Coating Particles on Glass

One end of a clean glass slide is taped on to the syringe pump such that the other of the slide is dipped into a beaker of de-ionized water. The whole set up is placed in a clean and airflow-free place. The set up is left as such to minimize disturbances from surface fluctuations. The water-air interface surface is lit externally using a fiber light for clear visualization. The particle colloidal suspension is slowly dispensed as droplets near the water-air interface such that the interface is not disturbed. The suspension is added till the surface of water is covered with particles which fluoresce under the fiber optic light. The syringe pump is set up to lift at the speed of 10ml/hr. The film at the water-air interface is transferred on to the glass slide when the vertically dipped glass slide is lifted by the syringe pump at the rate of 10ml/hr. As the film is transferred on to the glass slide the solvent evaporated leaving a film of 200nm particles

on the glass surface which is untaped from the syringe pump and used for subsequent processing.

Preparation of PDMS Master Template

A schematic outline of the procedure is shown in Figure 3-1. The self-assembled particles on glass substrate can be easily transferred to a poly(dimethylsiloxane) (PDMS Sylgard 184, Dow Corning) mold. Poly (dimethylsiloxane) (PDMS, Sylgard 184, Dow Corning) precursors were mixed in various ratios and examined for flexibility and better embedding of the nanoparticles. The ratios varied tried were of 7:1, 8:1, 9:1, and 10:1. It was found that 9:1 ratio mixture had the desired qualities as it was easy to peel, flexible and easily embedded the particles on to it. The flexibility of PDMS is crucial as it helps in the creation of microstructured mold on both planar and curved regions of the glass substrate. The mixed Poly(dimethylsiloxane) (PDMS, Sylgard 184, Dow Corning) was degassed to remove air bubbles and then poured over the dip coated nanoparticles supported by the glass substrate. The mixture was then subjected to curing in a hot air oven at 80 °C for 30 min. The solidified PDMS mold was gently peeled off the dip coated glass slide. This process is repeated to make as many templates as desired. Here we shall consider that we have made two PDMS molds so that they can be subjected to two different methods of fabrication – one with etching and one without etching.

Fabrication of Anti Reflection Coating (Hemispherical) Without Chemical Etching

Ethoxylated trimethylolpropane triacrylate(ETPTA, SRS454) is mixed with its initiator to form a mixture that can be polymerized under UV. The mixture is spin coated on to clean glass slides using a spin coating set up of 6000rpm for 20s. The speed of the spin coater and the duration of spinning can be varied as desired. The spin coating generally

forms a coating of thickness ranging from a few micrometers to a few nanometers. The PDMS mold with particles embedded is carefully placed on the spin coated ETPTA supported on a glass substrate. A gentle pressure is applied manually and the ETPTA monomer is polymerized using Xenon pulsed UV curing system for 4s. After the curing the PDMS mold is slowly peeled off. The PDMS mold can be used as a master for making 200nm features multiple times by simply rinsing the PDMS mold with ethanol.

The same process can be repeated on the other side of the glass substrate to make double sided antireflection coating.

Fabrication of Anti Reflection Coating (Hemispherical) After Chemical Etching

The PDMS mold surface embedded with 200nm particles is chemically etched to remove the particles so as to get dimple structures on the PDMS. The etching solution used is 2% hydrofluoric acid aqueous. The PDMS mold is dipped in 2% hydrofluoric acid aqueous solution for 25 min to ensure complete removal of particles. Then the above steps used for fabricating the antireflection coating without etching is repeated using the etched sample to get nipple arrays similar to that of moth corneas. Similar to the previous method the PDMS mold can be rinsed and used again to make 200nm features.

Antireflection Coating Fabrication with Spherical Voids

A schematic outline of the process is shown in figure 3-2. Two glass slides dip coated with 200nm silica particles are used. The slides are aligned parallel to each other as shown in the figure. They are separated with spacer blocks made of Teflon. A polymer mixture consisting of ETPTA and Polyethylene Glycol Diacrylate (PEGDA) is poured into the gap between the two dip coated glass slides and polymerized using Xenon pulsed UV curing system for 4s. The polymerized coating is peeled off from the

glass slides and spacer set up and etched using a 2% hydrofluoric acid aqueous solution for 2 hrs to ensure complete removal of particles.

Measurement and Analysis

The optical reflectivity of the samples formed with and without etching is evaluated using visible and near-IR reflectivity measurement at normal incidence. Reflectance of the samples is measured using an Ocean Optics HR4000 high resolution fiber optic UV-visible-near-IR spectrometer. The reflectivity is calibrated using a STAN-SSL low-reflectivity reflectance standard from Ocean Optics. The sample is illuminated using a halogen lamp and the beam's spot size formed on the sample was measured to be about 5mm. Absolute reflectivity is calculated as the ratio of the sample spectrum and the reference spectrum. An aluminum-sputtered (500 nm thickness) silicon wafer is used as reference. Multiple spots on the sample are measured for reflectivity and the readings are averaged. This average gives the absolute reflectivity. Similarly transmission readings are taken and the control is chosen to be a clean glass slide.

Results and Discussion

Figures 3-3 A and B show the SEM images of 200nm voids. The images show that the coating is uniform across the film and the voids are completely formed. The graph shown in Figure 3-4 is the transmission spectra for the antireflection coating and it can be seen the transmission percentage keeps increasing as the wavelength increases from 400nm to 900nm. At around 85nm it reached a maximum transmission of 97%

Figure 3-5 shows the transmission spectra for antireflection coatings of etched samples and samples that were not etched. The figure is interspersed with noise signals and was subjected to signal processing to get Figure 3-6. Figure 3-6 shows the

transmission spectra without any noise. This clearly shows that the glass slides having antireflection coatings on both sides have a higher transmission percentage compared to the control. It is to be noted that these sample are not etched and were fabricated with PDMS molds with particles embedded on their surface. The three samples A, B and C have transmission of 97% to 98% at around 650nm to 900nm. The samples with film on one side showed relatively lower transmission compared to the samples coated on both sides. But still the transmission was higher than the control and was around 95% to 97%. The sample coated using etched PDMS mold showed relatively better transmission than the control but the values were not significant enough. When this spectra is compared with the spectra of samples with spherical void samples it can be seen that the spherical void containing samples and slides coated on both sides with films have similar transmission percentage values

Reflection spectra of the samples are shown in Figure 3-7. The control shows very high reflectivity. Complementing the transmission spectra the three samples coated on both sides show very low reflection. Comparing the single side coated samples, samples that were prepared with PDMS that had particles embedded on to its surface shows a slightly better antireflection than the sample that was prepared with etched

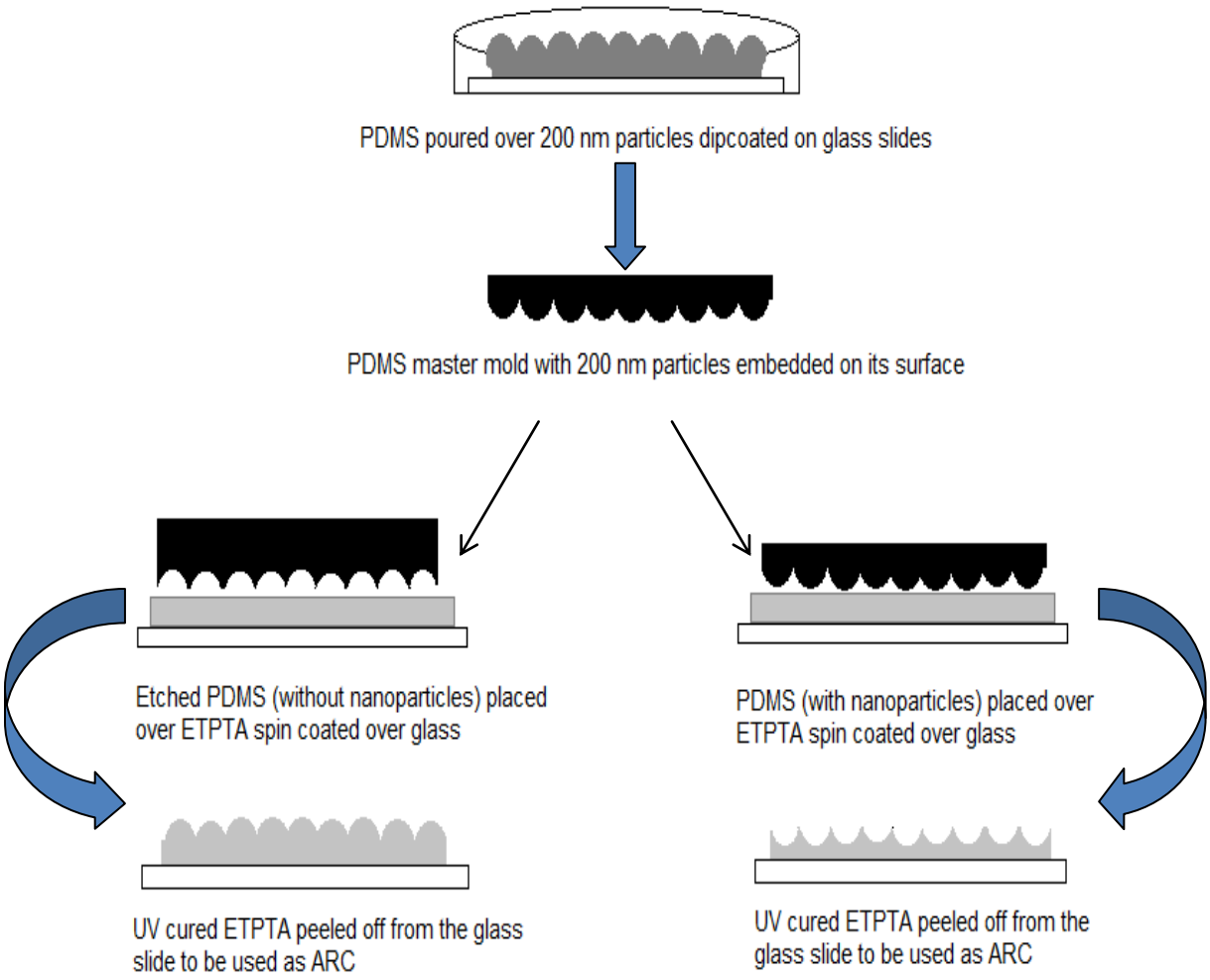

Figure 3-1. Fabrication of antireflection coatings - hemispherical

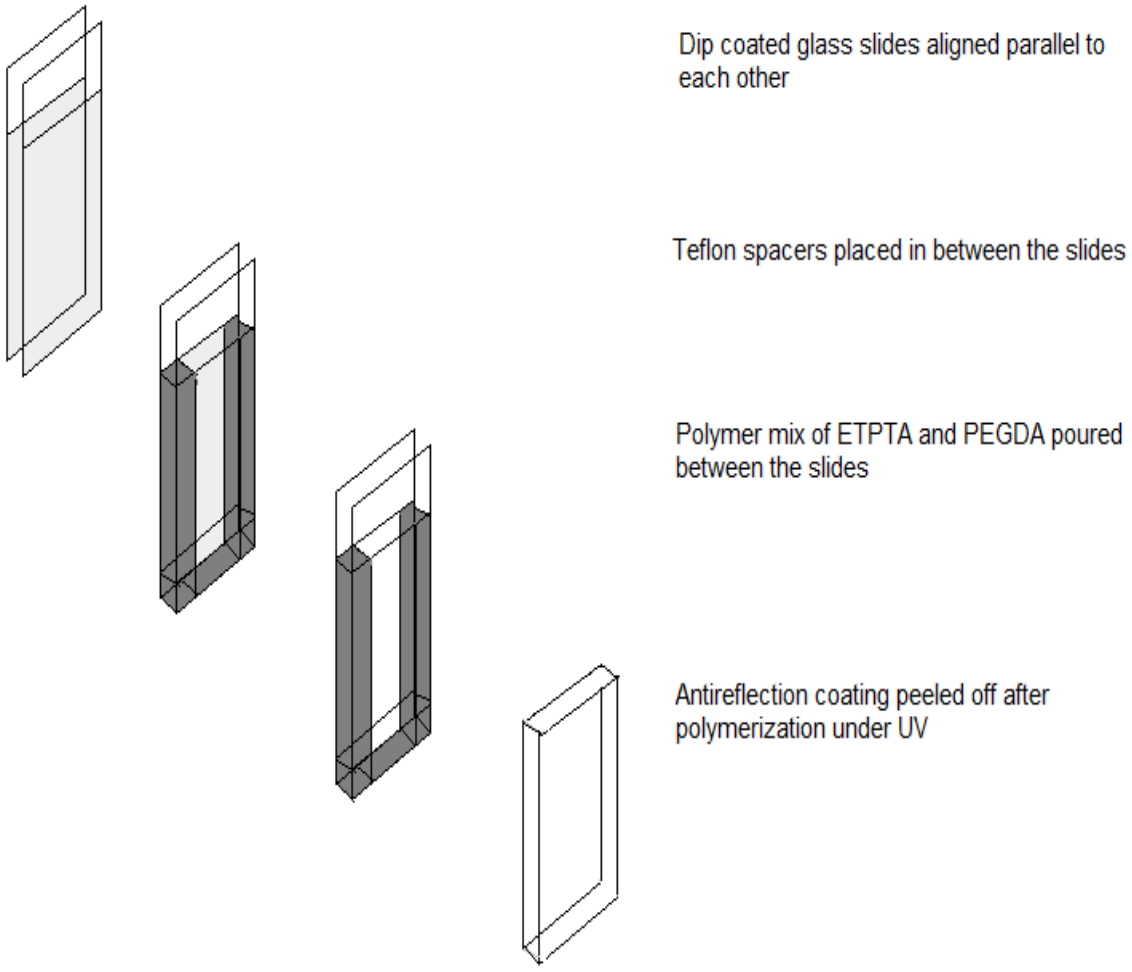

Figure 3-2. Fabrication of antireflection coating (Spherical voids)

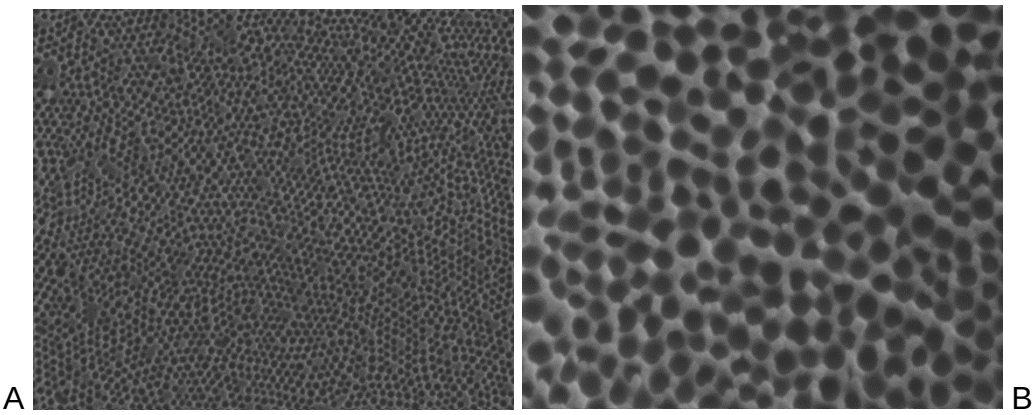

Figure 3-3. SEM Images of antireflection coating with spherical voids. A) SEM image showing 200nm spherical voids, B) Magnified image of 200nm voids.

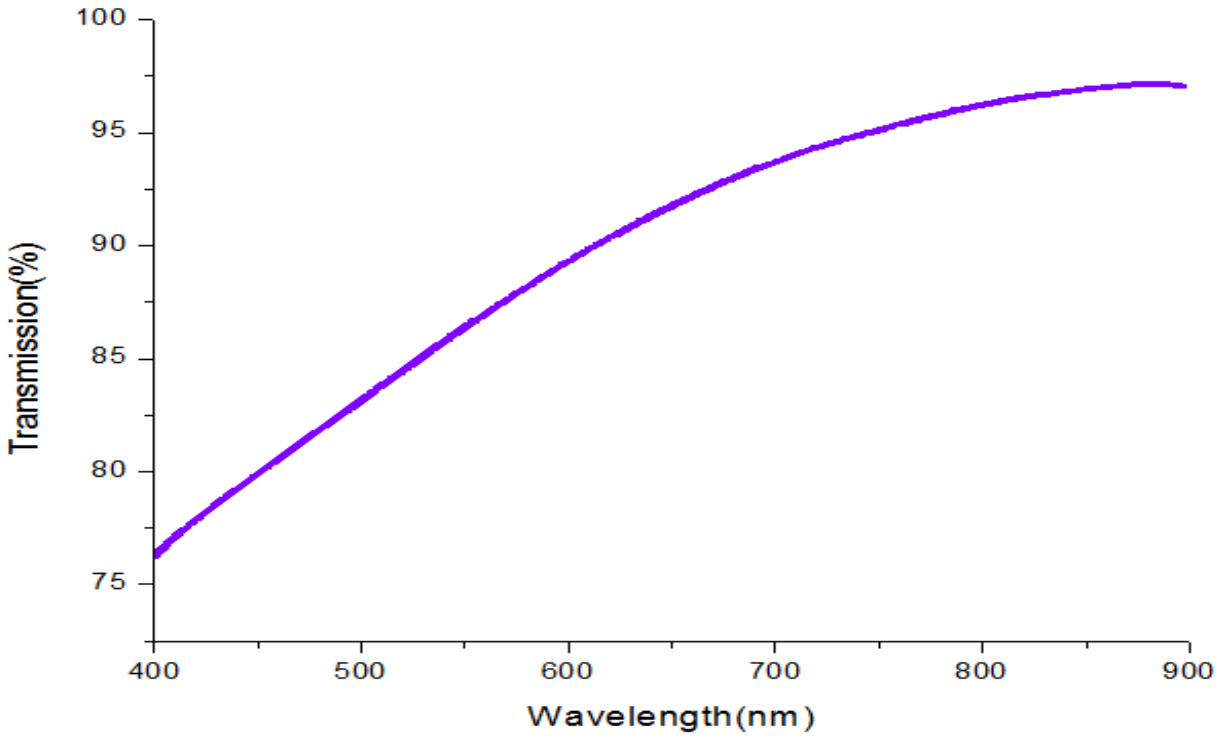

Figure 3-4. Graph depicting transmission spectra of antireflection coating (spherical voids).

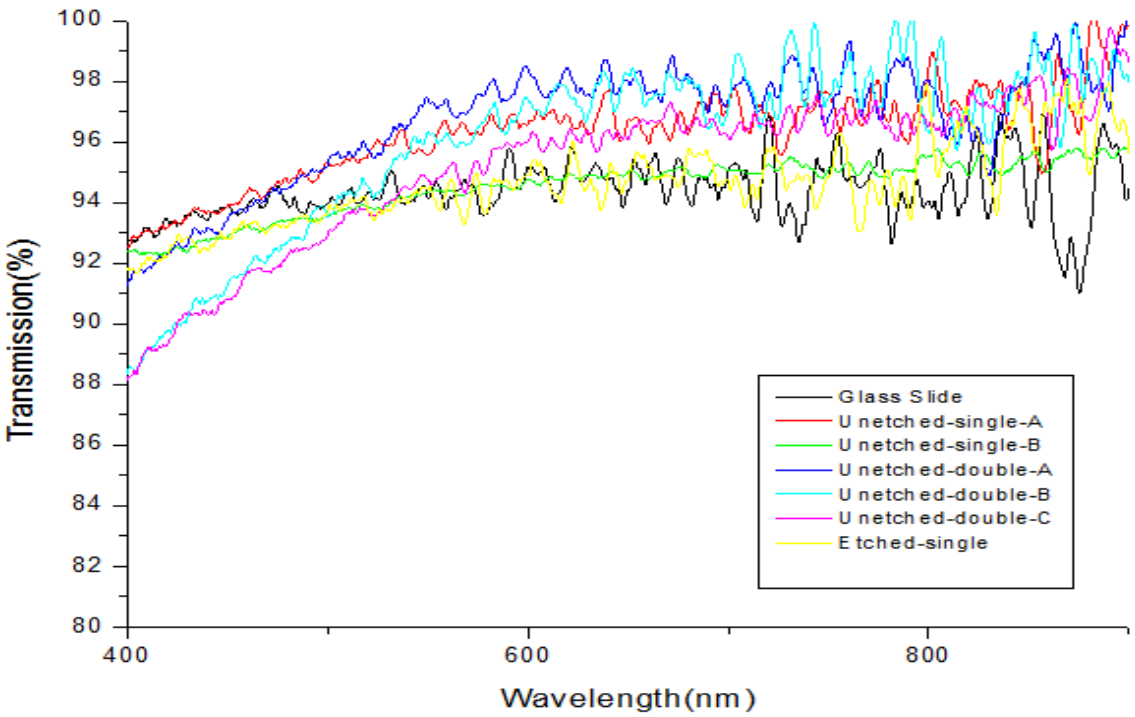

Figure 3-5. Transmission spectra of antireflection coating with noise (hemspherical voids).

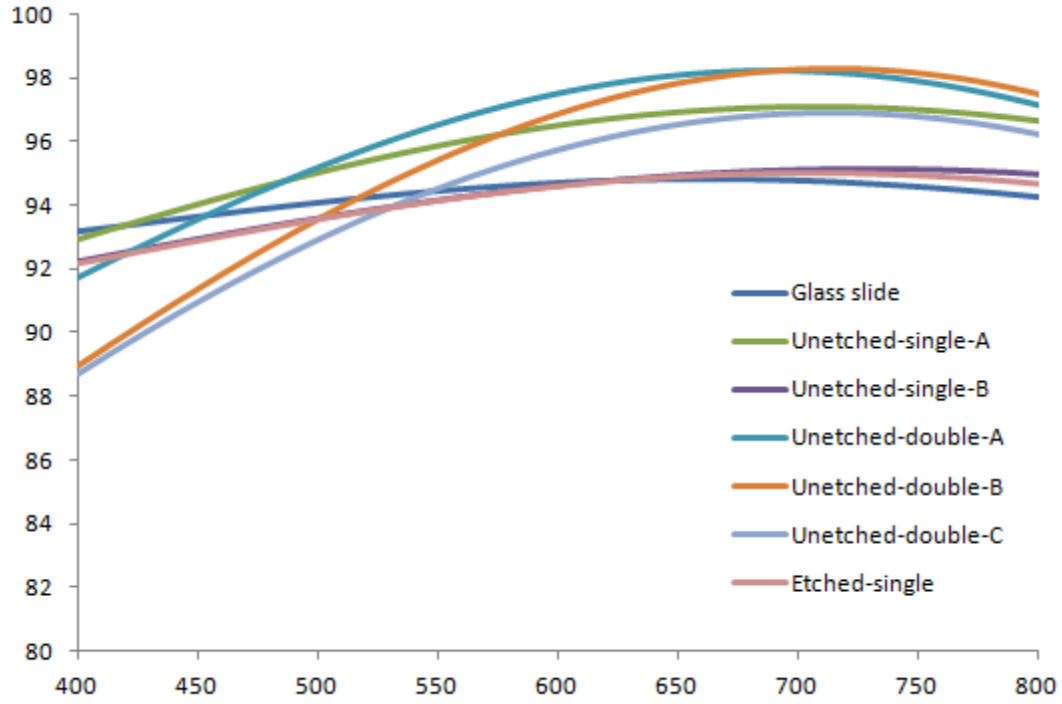

Figure 3-6. Transmission spectra of antireflection coating after removal of noise signals (hemspherical voids).

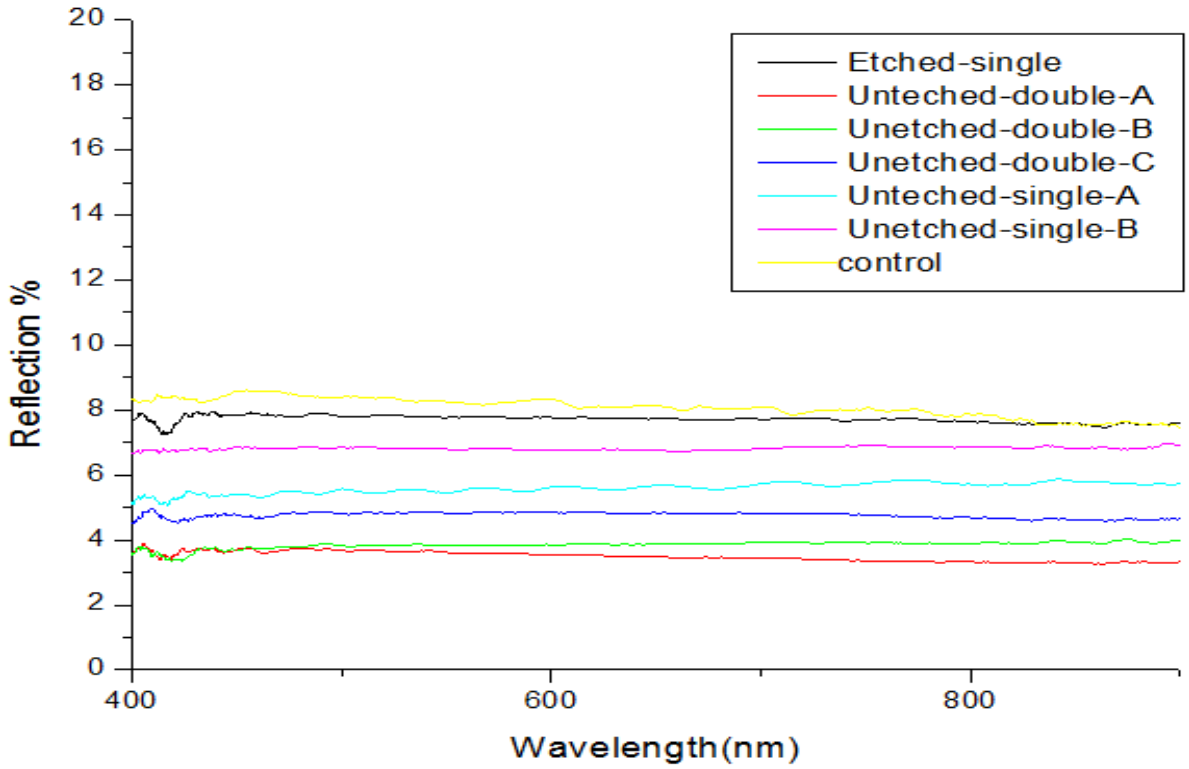

Figure 3-7. Reflection spectra of antireflection coating (hemspherical voids).

CHAPTER 4
CONCLUSION

Two different research projects associated by the method of floating assembly were reported. In the first part, yeast cells were coated on to glass exploiting their property to form a floating cell assembly on the air-water interface in a low concentration colloidal system. In the second part 200nm particles, dip coated using a similar floating assembly, were used to fabricate antireflection coatings.

The first part reported is for fabricating yeast coatings using simple dip coating technique. 20%, 30% and 40% yeast suspensions were coated once, twice and thrice and the optical microscope images were analyzed using 'ImageJ'. It was found that the coatings got better as the number of coatings and the concentration increased. But slides coated with 30% yeast solution once had better percentage coverage than slides coated with 40% yeast solution once. There were few regions with multiple layers as the concentration of the solution increased. The monolayers thus produced have a variety of applications in research and diagnostics.

In this project an easy and scalable antireflection coating fabrication was reported using a simple floating assembly of nanoparticles and exploiting the self assembly characteristic of the nanoparticles. Close packed 200 nm colloidal particles were coated on a glass substrate using simple dip coating process. The resulting coating was embedded on poly(dimethylsiloxane) (PDMS) by casting them as molds. The master PDMS molds were used in two different ways. In the first method the embedded nanoparticles were used to cast dimple structures on poly(ethoxylated trimethylolpropane triacrylate) (PETPTA). The ethoxylated trimethylolpropane triacrylate (ETPTA) was spin coated on to glass slides for support and polymerized by ultra violet

radiation. In the second method the silica nanoparticles were removed by chemical etching and then the voids in the PDMS molds are used to cast nipple structures on ETPTA which is later polymerized as before. Glass slides were coated on single side and double side to check the antireflection properties of the nanostructures. These were compared with antireflection coatings produced to have spherical voids. The antireflection coatings produced were analyzed to get reflection and transmission spectra. The double sided coatings that were fabricated without etching showed the best results with low reflection and high transmission. The single sided unetched coating and the coating with spherical voids showed relatively good antireflection property. These biomimetic antireflection coatings thus fabricated can be applied for different purposes ranging from simple LCD screen coatings to solar panels.

Yeast cell coatings will be tested to show that the procedures did not in any way damage the cells. The procedure can be extended to optimize the coating conditions for other biomolecules and organisms.

A simulation will be run for the antireflection coatings fabricated. Since moth eye antireflection structures are sub-300nm, the same processes can be applied to 100nm and 300nm particles and the films thus obtained can be subjected to optical measurements to check if they perform better than the coatings fabricated under this research project. During the experimentation sessions it was seen that sometimes ETPTA can be easily peeled off. So the thickness of the membranes can be optimized to check whether easily peel-able membranes can be fabricated.

LIST OF REFERENCES

(1) Tang, Z., Zhang, Z., Wang, Y., Glotzer, S.C., Kotov, N.A. *Science* **2006**, 314, 274-278

(2) Yuanfang Liu, Shaopeng Wang, Jung Woo Lee, Nicholas A. Kotov. *Chemistry of Materials* **2005,** 17, 4918-4924

(3) Alivisatos, A. PaulJohnsson, Peng, Xiaogang, Wilson, Troy E., Loweth, Colin J., Bruchez, Marcel P., Schultz, Peter G. *Nature* **1996** 382, 609 – 611

(4) Venugopal Santhanam, Jia Liu, Rajan Agarwal, and Ronald P. Andres. *Langmuir* **2003,** 19, 7881-7887

(5) Katsuhiko Ariga, Jonathan P Hill, Michael V Lee, Ajayan Vinu,, Richard Charvet , Somobrata Acharya. *Science and Technology of Advanced Materials*.**2008** 9, 96

(6) Prevo, B. G.; Fuller, J. C.; Velev, O. D.*Chemistry of Materials*. **2005**, 1728–35.

(7) Kuncicky, D. M.; Christesen, S. D.; Velev, O. D. *Applied Spectroscopy* **2005**, 59,401–409

(8) Lee, J. A.; Meng, L. L.; Norris, D. J.; Scriven, L. E.; Tsapatsis, M. *Langmuir,* **2006**, 22, 5217–5219

(9) Frank Caruso and and Corinna Schüler *Langmuir* **2000** 16 (24), 9595-9603

(10) Mi-Kyoung Park, Ken Onishi,†, Jason Locklin, Frank Caruso, Rigoberto C. Advincula *Langmuir* **2003** 19 (20), 8550-8554

(11) A. Pandit, H. de Groot, A. Holzwarth, *Harnessing Solar Energy for the Production of Clean Fuels*, Leiden Institute of Chemistry, The Netherlands,2006.

(12) A. Melis, L. Zhang, M. Forestier, M.L. Ghirardi, M. Seibert**,** *Plant Physiology*. **2000** 122: 127-136.

(13) M.L. Ghirardi, A. Dubini, J. Yu, P.-C. Maness, *Chemical Society Review* **2009,** 38, 52.

(14) Kahraman, M.; Yazici, M. M.; Sahin, F.; Culha, M. *Langmuir* **2008,** 24,894–901

(15) A. Melis, L. Zhang, M. Forestier, M.L. Ghirardi, M. Seibert, *Plant Physiology* **2009,** 122-127.

(16) Fidaleo, S. Charaniya, C. Solheid, U. Diel, M. Laudon, L.E. Scriven, M.C.

Flickinger, *Biotechnol. Bioeng*. **2006,** 95, 446.

(17) M. Fidaleo, M.C. Flickinger, *J. Chem. Eng. Sci*. **2011,** 66 3251

(18) Jeong, K. H.; Kim, J.; Lee, L. P. *Science* **2006,** *312*, 557.

(19) Vukusic, P.; Sambles, J. R. *Nature* **2003**, *424*, 852.

(20) Aizenberg, J.; Muller, D. A.; Grazul, J. L.; Hamann, D. R. *Science* **2003,** *299*, 1205. 104

(21) otyrailo, R. A.; Ghiradella, H.; Vertiatchikh, A.; Dovidenko, K.; Cournoyer, J. R.; Olson, E. *Nature Photonics* **2007**, *1*, 123.

(22) Stavenga, D. G.; Foletti, S.; Palasantzas, G.; Arikawa, K. *Proceedings of the Royal Society B-Biological Sciences* **2006**, *273*, 661.

(23) Walheim, S.; Schaffer, E.; Mlynek, J.; Steiner, U. *Science* **1999**, *283*, 520.

(24) Hiller, J.; Mendelsohn, J. D.; Rubner, M. F. *Nature Materials* **2002**, *1*, 59.

(25) Ibn-Elhaj, M.; Schadt, M. *Nature* **2001**, *410*, 796.

(26) Xi, J. Q.; Schubert, M. F.; Kim, J. K.; Schubert, E. F.; Chen, M. F.; Lin, S. Y.; Liu, W.; Smart, J. A. *Nature Photonics* **2007**, *1*, 176.

(27) Prevo, B. G.; Hwang, Y.; Velev, O. D. *Chemistry of Materials* **2005**, *17*, 3642

(28) Madou, M. J. *Fundamentals of Microfabrication: The Science of Miniaturization; CRC, Boca Raton, FL,* **2002**

(29) Ozin, G. A.; Arsenault, A. C. *Nanochemistry: A Chemical Approach to Nanomaterials;* RSC, Cambridge **2005**.

BIOGRAPHICAL SKETCH

Hemalatha Velavan has a bachelor's degree in Biotechnology from SRM University, Chennai, India. She has worked as an intern in many reputed institutions and research centers. She is interested in bioprocess engineering and nanofabrication. She worked as a part time technical assistant at ICBR/CGRC and as a volunteer research assistant in the Department of Pharmacology at UF during the course of her graduate degree in chemical engineering. She graduated from the University of Florida in May 2013 with a master's degree in chemical engineering with a strong focus in material science and engineering.